ALMYROS 2

Archaeological Background

The magoula named "Almyros 2" is located 2 km south of the modern town of Almyros. Wheat and corn are predominantly cultivated on the site today. No archaeological excavations have been carried out at the prehistoric settlement. However, field surveys have been made by the IG' EPKA and the Netherlands Institute (1992 - 1997). According to the surface finds, including ceramics, the settlement that existed here spanned the Early Neolithic to the Middle Neolithic period (6800-5300 BCE).

The landscape around Almyros 2 is diverse and characterized by flat agricultural floodplains, large river and stream beds that produce deep gorges, and mountains on the southern periphery. The modern towns of Almyros and Efxeinoupoli are some 1.5 km to the north of the target area. The National Road passes along the eastern periphery at a distance of 4 km and the modern coastline is nearly 9 km away. The landscape rises gradually from east to west. Almyros 2 is positioned squarely within the floodplain. Most of the agricultural fields appear to be used for wheat and corn cultivation. The harvest appears to have been recently completed in the 4 June 2012 WorldView-2 and most of the fields around the site have no vegetation. Elevations around the target site range from 85-95 masl.

Satellite Remote Sensing and Historical Aerial Photography Survey

A WorldView-2 image from 4 June 2012 was used for satellite remote sensing at Almyros 2 (Figure 1). The satellite image has an off-nadir angle of 21.6° and a ground sampling distance (GSD) of 0.55 m (panchromatic and 2.11 m multispectral. In addition to the satellite imagery, four aerial photographs were used for remote sensing: (1) 1945 (date unknown) with a scale of 1:42000; (2) 1960 (date unknown) with a scale of 1:30000; (3) 1971 (date unknown) with a scale of 1:18000; and (4) 30 July 2003 with a scale of 1:30000 (Figure 2).

The aerial photographs proved useful in monitoring 20th century environmental and land use changes around the prehistoric settlement (Figure 3). The 1945 photograph documents a number of streams in the region that fed into the large river 800 m to the north. Most of these streams are no longer water channels. Some have been filled up and converted into agricultural fields or their courses have been redirected into canals. These changes occurred sometime in the 1950s and 1960s, since the 1971 photograph shows the transformation being complete. Some of the stream beds, although covered up, are still visible as soil marks in the 1971 photograph. Even less are noticeable in the 4 June 2012 WorldView-2 image. In sum, a comparison of the aerial photographs and the satellite image indicates that the Almyros 2 was close to water sources at an earlier period. One stream bed appears to have been approximately 100 m north of the prehistoric settlement.

Satellite remote sensing within a 1 km radius around Almyros 2 produced modest results (Figures 4-5). The majority of features correspond to palaeochannels (blue) associated with the rivers and streams that once pocketed the terrain. High concentrations of palaeochannels appear immediately north and east of the prehistoric tell. Nearly all of these are now agricultural fields with little evidence of past hydrological activity. Therefore, at some time in the past, the area of Almyros 2 had close access to water sources. Other anomalies relate to agricultural activity (brown), such as former field divisions and plow lines. A third category of anomalies is unclassified (yellow). A few of these (e.g. #51-55) are globular and roughly circular formations that likely relate to previous hydrological activity, i.e. areas where water has flowed or settled as seasonal lakes. Anomaly #54 seems to be associated with the prehistoric tell (Figure 6). It is roughly circular and measures around 70 m in diameter. No other anomalies in the target area appear to be from obvious archaeological features.

Figure 1. Almyros 2 from a 4 June 2012 WorldView-2 image

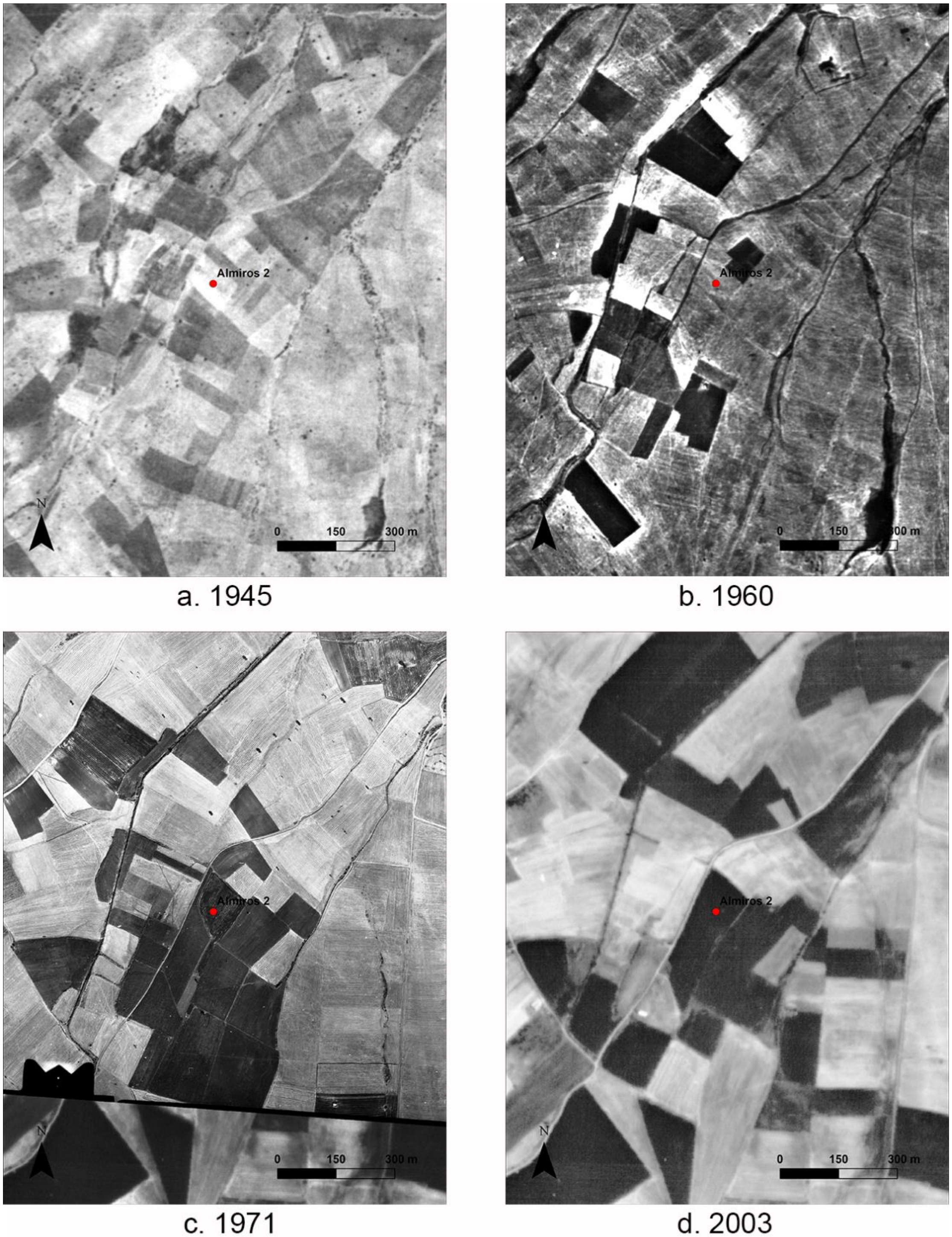

Figure 2. Aerial photographs of Almyros 2: (a) 1945; (b) 1960; (c) 1971; (d) 30 July 2003

Figure 3. 1945 aerial photograph (left), and 1971 aerial photograph (right) of Almyros 2. The courses of rivers and streams are visible in the 1945 photograph (red arrows), but they have been converted into agricultural land or canals by 1971

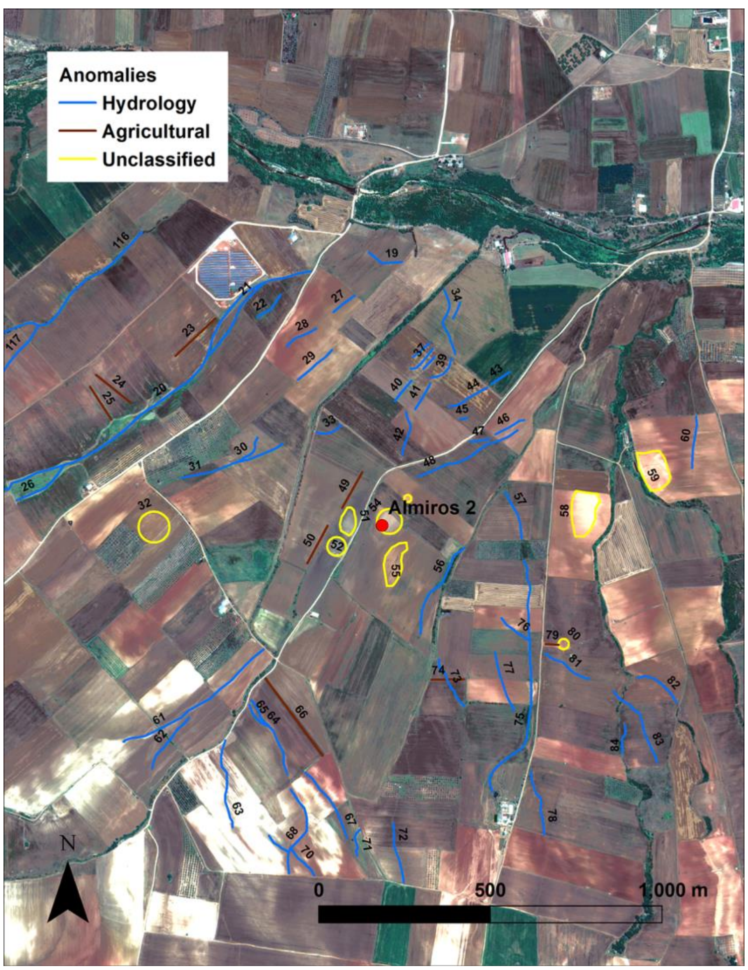

Figure 4. Surface anomalies from the 4 June 2012 WorldView-2 image within a 1 km radius around Almyros 2

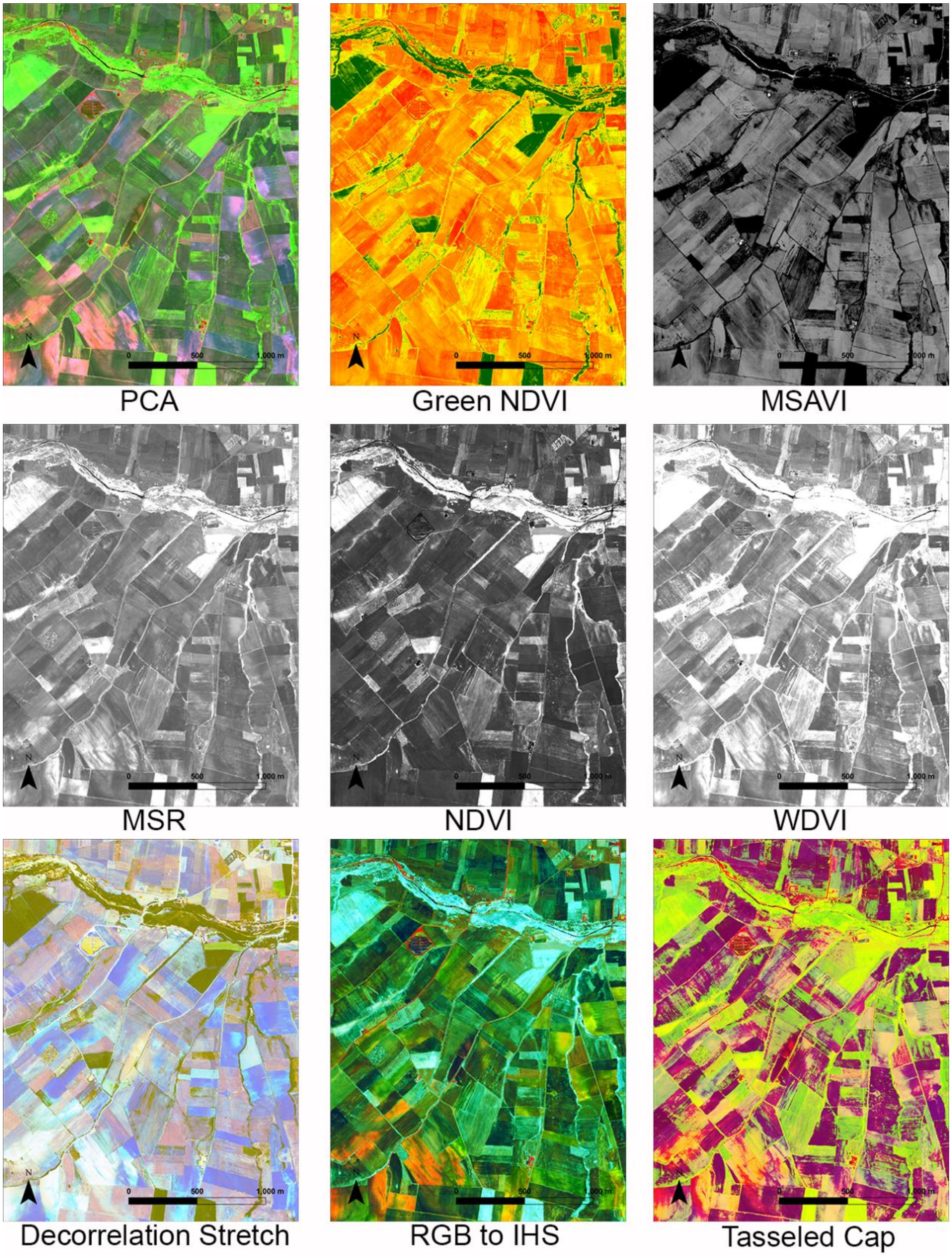

Figure 5. Spectral filters and vegetation indices applied to the 4 June 2012 WorldView-2 image around Almyros 2

Figure 6. PCA of the 4 June 2012 WorldView-2 image of Almyros 2 showing a roughly circular anomaly that marks the location of the prehistoric tell

Remotely Piloted Aircraft Systems (RPAS) Survey

As with the other magoules, the field conditions were not optimal for air-photo-interpretation at Almyros 2. Indeed, the magoula spreads between three field-plots: one has been plowed recently, the other still has wheat residues from recent harvesting, and the third one has traces of burned corn husks.

The two harvested fields (the Northern and Southern ones) are practically not "readable" from the photo-interpretation point of view. The middle one is also quite hard to read, but it provides same vague clues of possible buried structures of sub-circular concentric shape (Figure 7).

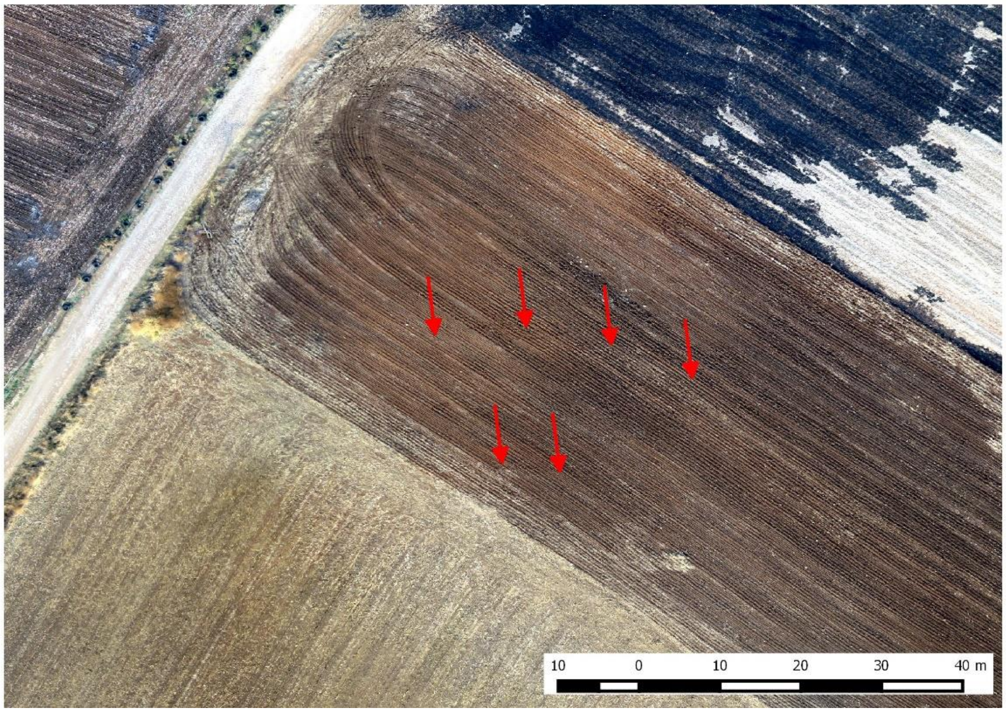

Figure 7: Sub-circular concentric linear features, potentially representing buried structures of the Magoula (November 10th, 2015)

Those traces, mostly of negligible importance on their own, make sense only when linked with the results from geophysics (Figure 8). Although a proper matching can be identified only for the smaller Southern trace of the two (see Figure 7), the general settings and orientation of both feature seems to follow the shape defined with geophysics.

The above identifications were only possible because of the good quality of the output ortho-photo, with a ground resolution of a few centimeters (despite some small areas of blurriness). The same level of detail could also be extracted for the digital terrain model (DTM), which, again in combination with geophysics, provided interesting information on the site.

Indeed, the northern side of Almyros 2 matches perfectly with the location of isolines derived from the photogrammetric DTM. The geomorphology of the area seems also to suggest a possible continuation of the magoula towards the South, where apparently another area shares the same top altitude of Almyros 2.

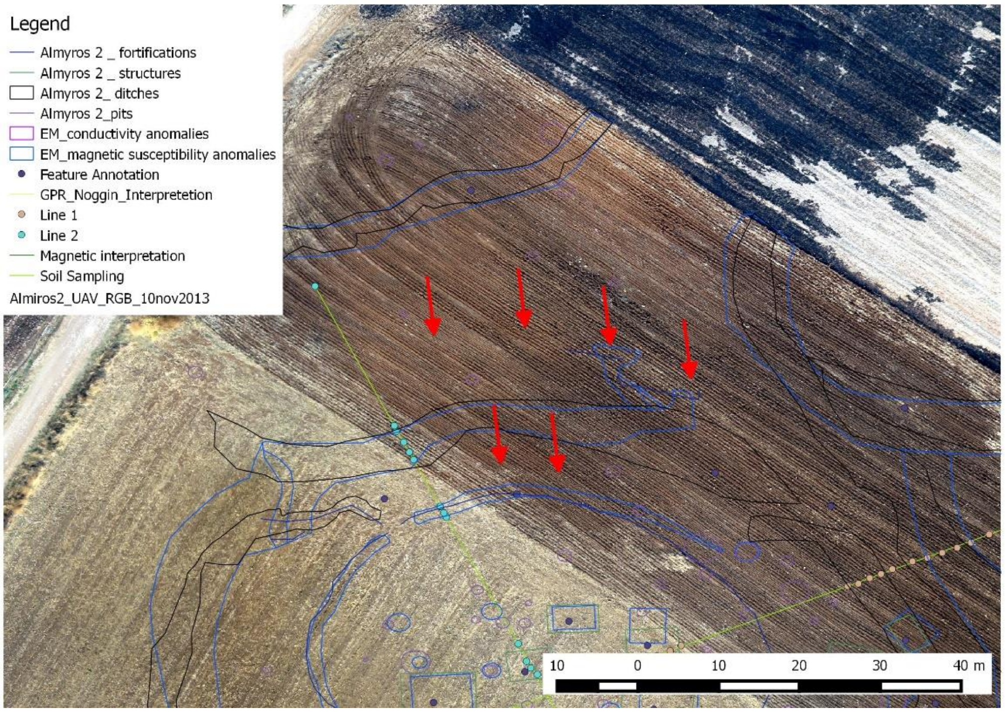

Figure 8: Linear traces from API (red arrows) and results from geophysics.

Another interesting confirmation on the presence of buried structures identified with geophysics comes from an examination of national orthophoto in the same area. Although the general halo of the circular magoula is mostly visible in all historical imagery provided by Google or Bing, the image from Ktimatologio shows a higher level of details and suggests the presence of multiple concentric linear structures (Figure 9).

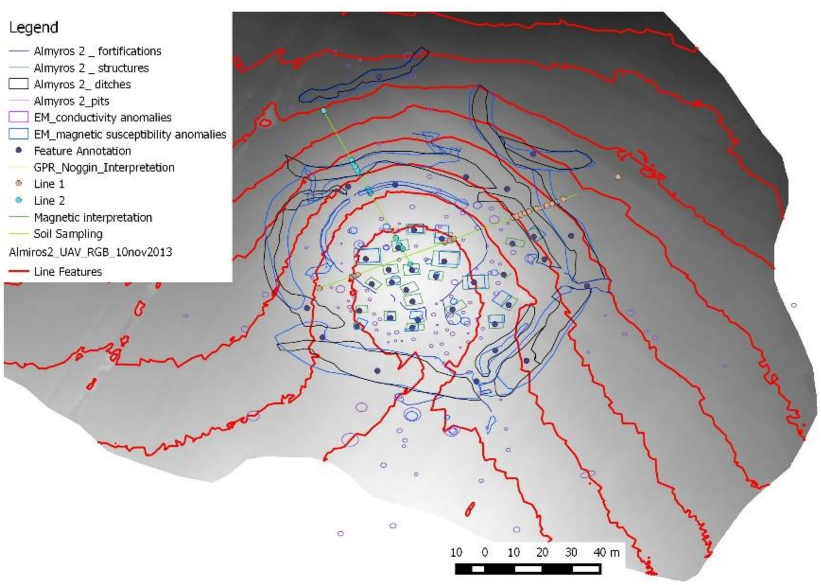

Figure 9: DTM in grayscale with isolines (red lines with 1 m altitude interval) and the geophysical results. Note the matching of the northern structures with the contourlines.

Figure 10: Matching between the geophysics and circular traces on the Ktimatologio orthophoto.

Geophysical Prospection

Geomagnetic Survey

The settlement is characterized by a wide enclosure, running around the core (A1, A3, A5, and A7). Another series of enclosures (A4 and A6) are located inside, supporting A3 and A5 in the eastern section. Considering the size and the signature of anomalies, these are most likely to be ditches. The anomaly A10, yet another enclosure located inside the settlement encircles the core of the settlement. This anomaly is thinner than others and has a stronger signature. C 1-5 are likely openings to the outside. Of additional interest is anomaly A9 where its circular shape (also evident in the satellite image) suggests a smaller settlement. However, considering the relatively large size of A9 with respect to the small-scale settlement it is bounding, one can suggest this “settlement” had some significant meaning to the habitants.

The buildings inside the ditches are spatially divided by the enclosure A10. It is not clear whether buildings inside A10 represent another occupational phase or if these structures had a special function or meaning in the social hierarchy of the community. It appears that buildings in the settlement were made of mudbrick (at least their superstructures) and they suffered from a burning event. However, it is not clear whether this event happened in a single phase or multiple phases. The “empty” zone within A10 also attracts some attention. This zone is devoid of the evidence for anthropogenic activities, already suggesting a deliberate action of continuous cleaning.

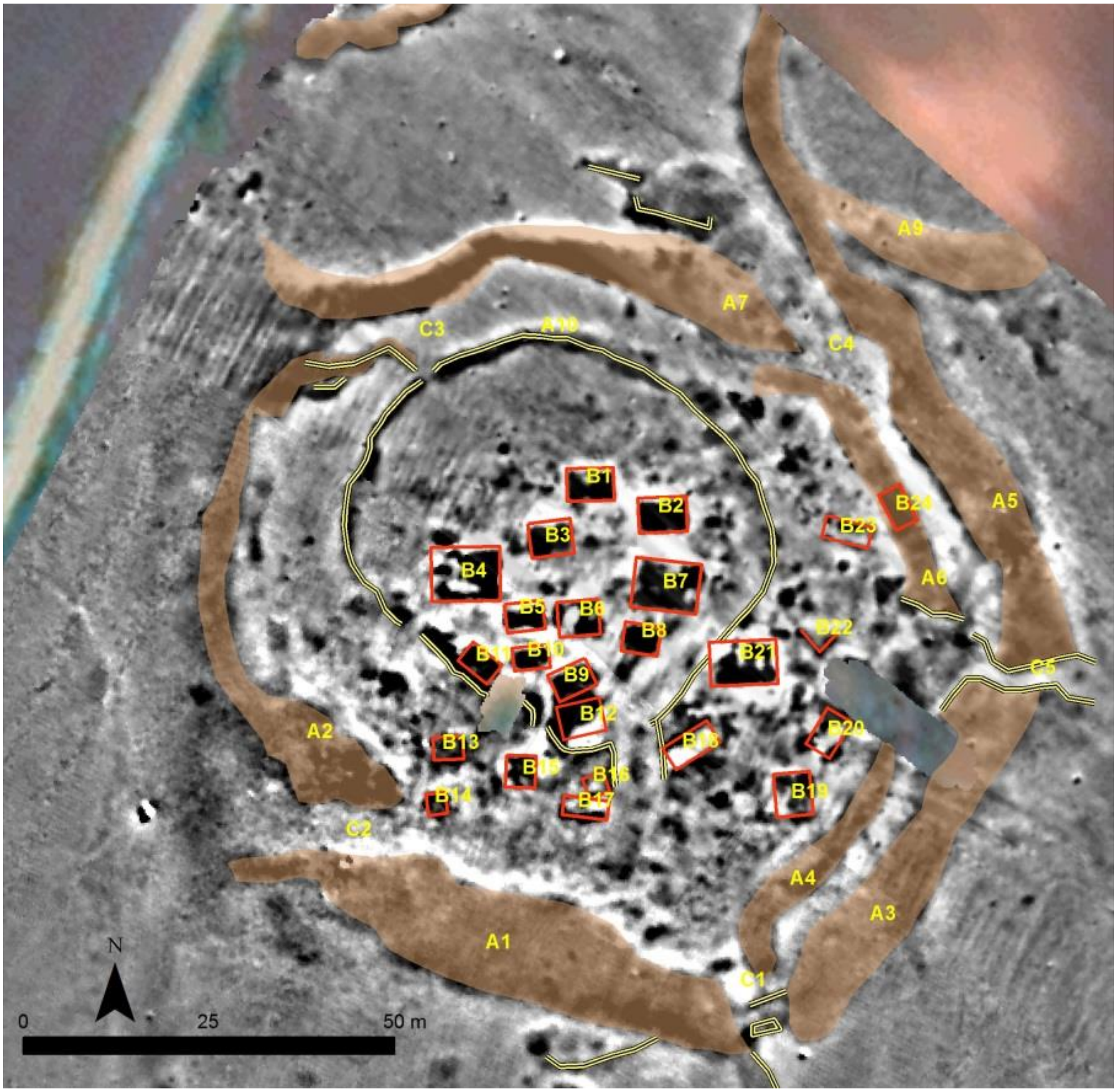

Figure 11: Results of the geomagnetic prospection with labeled anomalies

Electromagnetic Induction Survey

EM measurements were done on the site of Almyros 2 with the GEM-2 from Geophex. It was used with a GPS unit, acquiring simultaneously the location of the point and the value of the EM field for five different frequencies (from 5 kHz up to 90 kHz). Only the two first frequencies were used to extract the raw signal value of magnetic susceptibility and electrical conductivity. As the coil spacing is 1.6 m, the depth of investigation for the electrical conductivity is 2.5 m and 1.6 m for the magnetic susceptibility. We covered an area of 2.37 ha with the EM, completed in two days by two surveyors.

Electrical conductivity shows a large dynamic range from 50 to 90 mS/m (Figure 12). The map can be divided in two parts, one at the north-east that is more resistive, the other at the south-west that is more conductive. This difference could come from a distinct treatment of the agricultural soil (ploughing, kind of crops, etc.) But at the same time this difference seems to come also from the geomorphology with higher clay content in the south than north.

The electrical conductivity reveals clearly the Neolithic magoula in the middle of the map by a higher conductivity (as it is the case for the most part of the surveyed Neolithic site). Also the tell presents different parts, one more resistive in the south (where the structural remains are denser – see the suggested magnetic anomalies B1-B12, B18, B21) and another one more conductive in the north, but still more conductive than the surrounding field. The tell is surrounded by a perfectly circular ditch 4 m in width (A7).

Any isolated features appear through the electrical conductivity. But it is interesting to check the small outgrowth in the south (to the east of B16 and B17) breaking the circular shape of the central resistive anomaly. We also see poorly discernable resistive anomalies in the south probably related to artificial constructions or disturbances (to the south of C1).

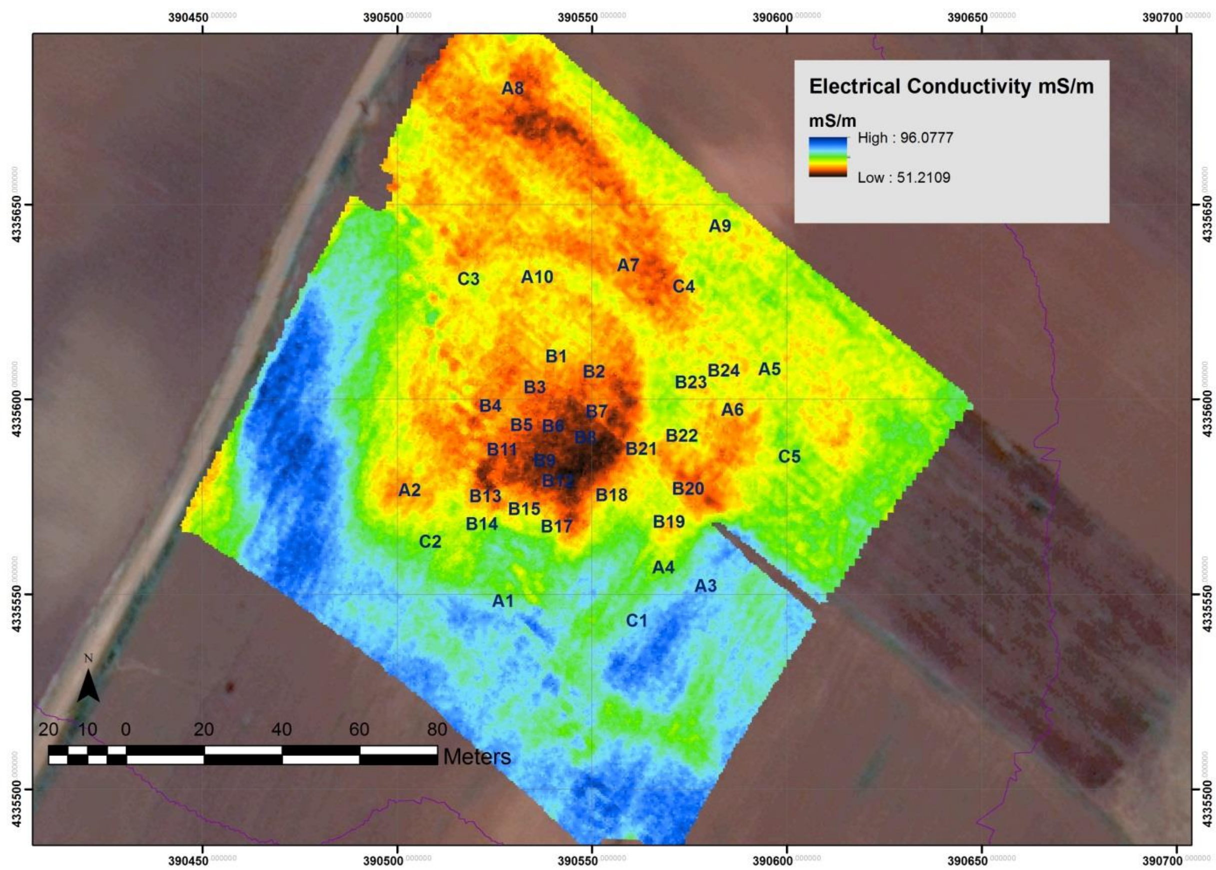

Figure 12: Apparent electrical conductivity (GEM-2: VCP)

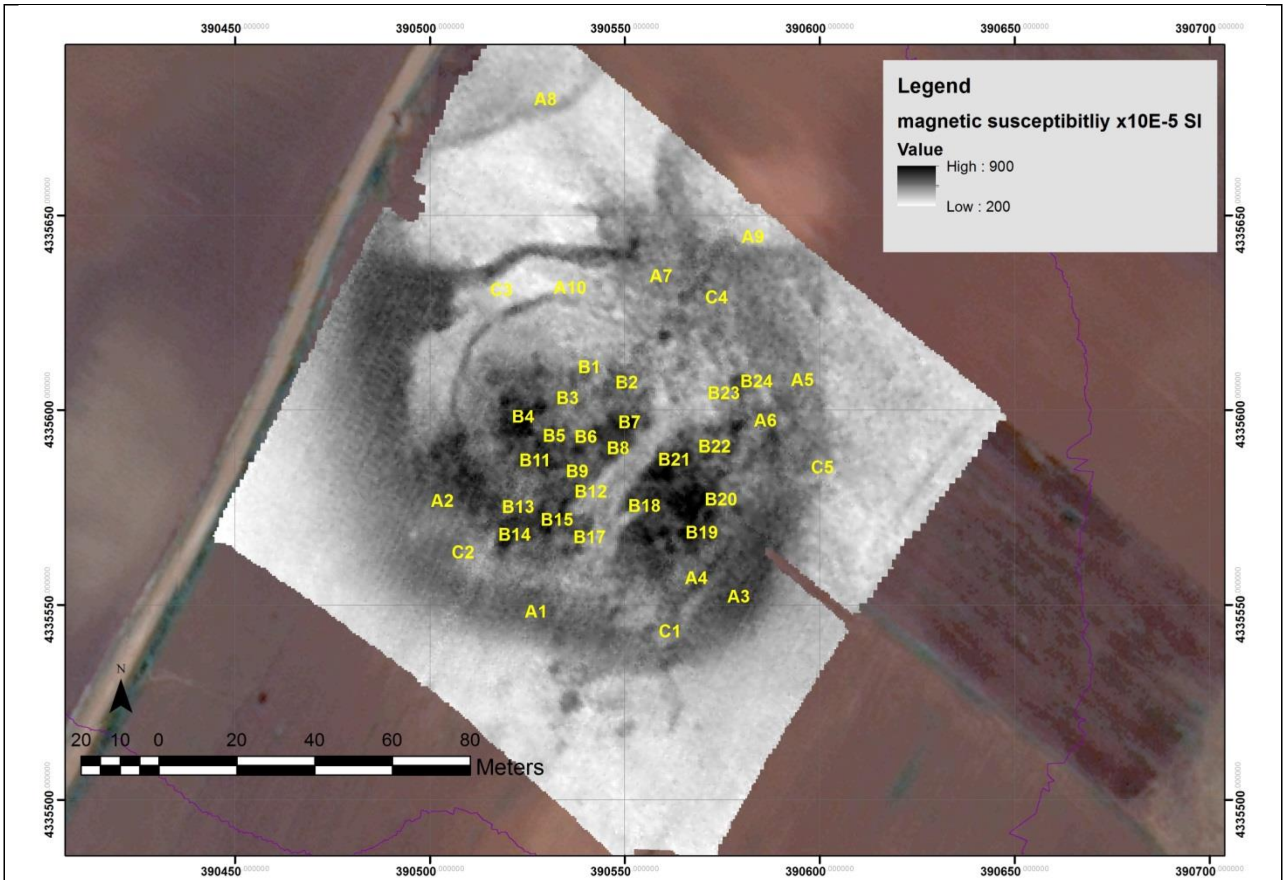

Figure 13: Apparent magnetic susceptibility (GEM-2: VCP)

The magnetic susceptibility shows a circular distribution around the magoula. Toward the north we can see two magnetic linear features. These ones correspond probably to ditches or walls. If the wider width of the northernmost (A7) signifies the location of a ditch, the inner one (A10) looks more like walls, despite the fact that both of them are strongly magnetic. Except for this part, all around the magoula we can observe several fuzzy anomalies (A6) increasing in terms of magnetization in the direction of the center of the magoula. These gradient anomalies could correspond to a flooding deposit. The increasing of the thickness of the deposit is probably directly related to the value of the magnetic susceptibility.

Inside the magoula we observe strong values of susceptibility in the south (corresponding also to the resistive values) and in good agreement to the magnetic data where we expect to have structural remains (features B#) and lower values in the north. This difference could reveal different kind of activities inside the magoula. On the top of the magoula we can observe a non-magnetic anomaly which does not appear on the electrical conductivity (the NE-SW lane that is defined between anomalies B8-B12-B15 and B17-B18-B21). This anomaly represents a specific area or a modern disturbance (such as a trench).

Figure 14 shows the magnetic susceptibility after processing to remove the global variation of the magnetic susceptibility and to enhance the local anomalies on the top of the magoula, but also all around the tell. In the extreme northern part of the survey area we can see two marks from a palaeochannel more visible on the magnetic susceptibility than on the electrical conductivity.

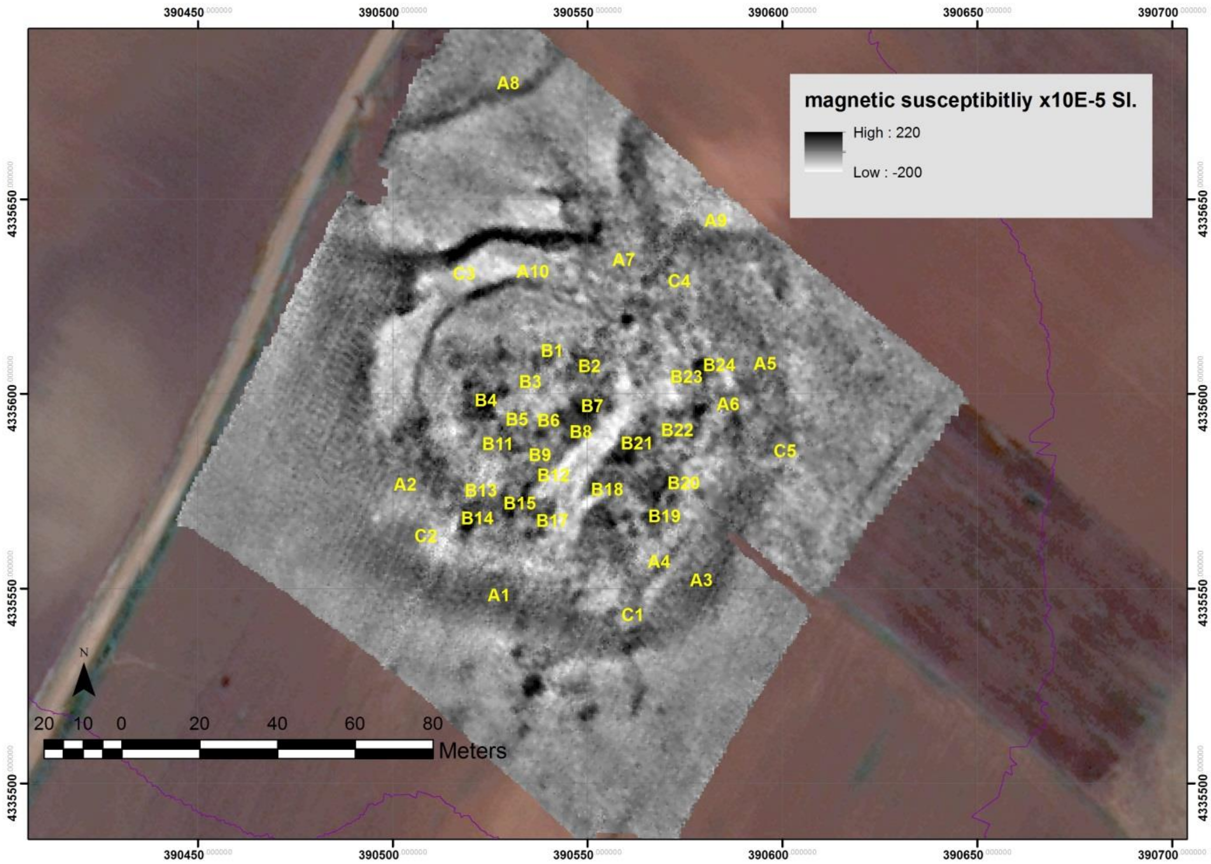

Figure 14: Processed apparent magnetic susceptibility (GEM2: VCP)

Ground Penetrating Radar Survey

The resulting GPR slices obtained by the single channel NOGGIN Plus Smart Cart at Magoula Almyros 2 are presented in Table 1. The area covered is 4250 sq m and consists of 5 grids that were set on the top of the magoula. The processing flow of this data set is: Trace reposition, Repick first break (20%), Dewow, SEC2 (Atn=24.29 dB_m,StrtG=3.32,MaxG=1096), Background average subtraction, Bandpass filter (Fc1=40 % Freq,Fp1=80 % Freq,Fp2=120 % Freq,Fc2=160 % Freq).

Overall, the results suffer from noise that was caused by crops on the surface, while the signals were significantly attenuated. As a result, the data are hard to interpret and for this reason magnetic results were used as guidance.

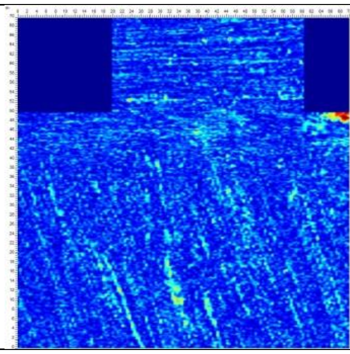	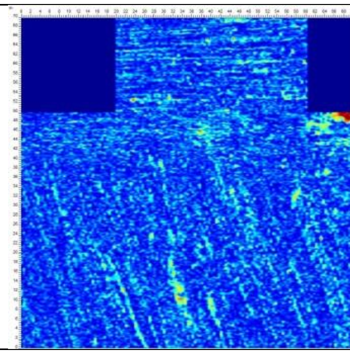	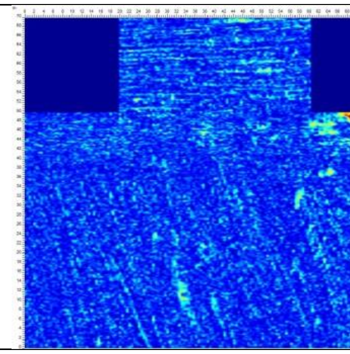
0-10cm	**10-20cm**	**20-30cm**
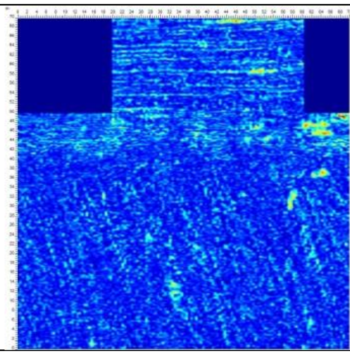	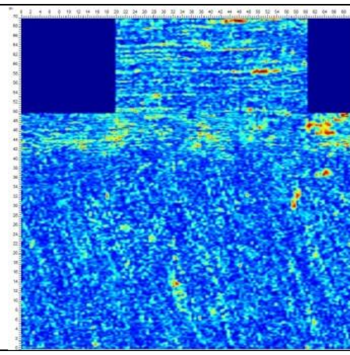	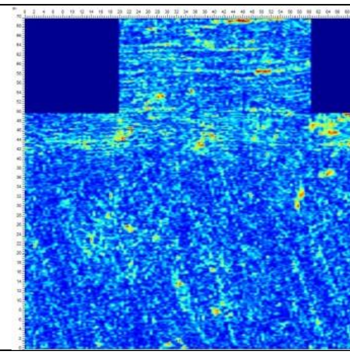
30-40cm	**40cm-50cm**	**50cm-60cm**
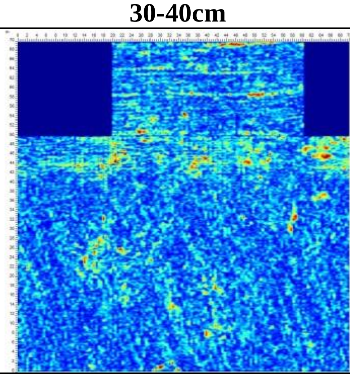	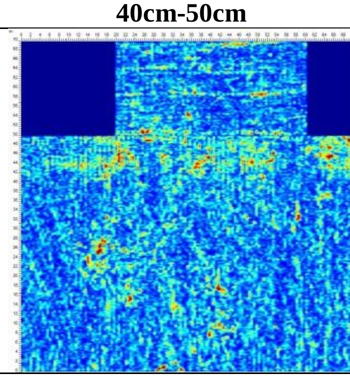	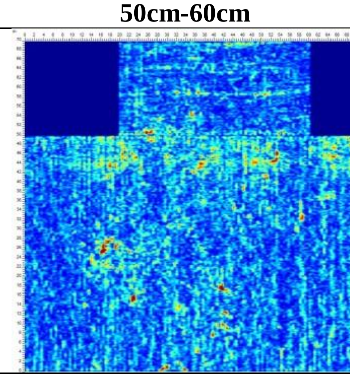
60cm-70cm	**70cm-80cm**	**80cm-90cm**
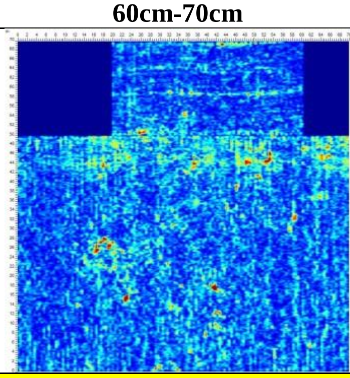	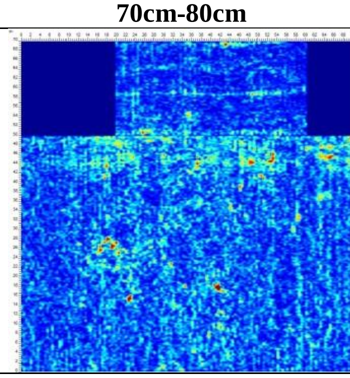	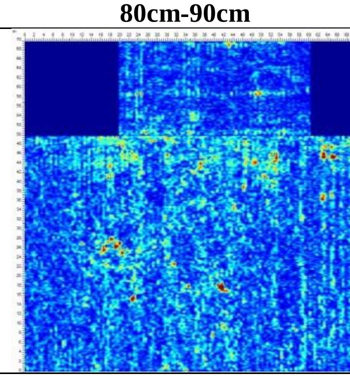
90cm-100cm	**100cm-110cm**	**110cm-120cm**

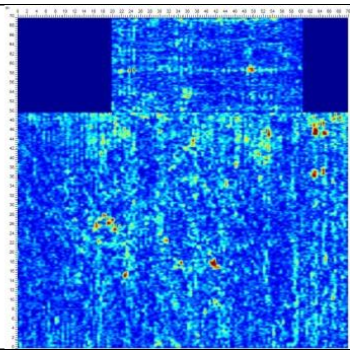	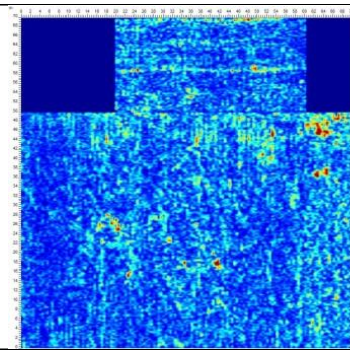	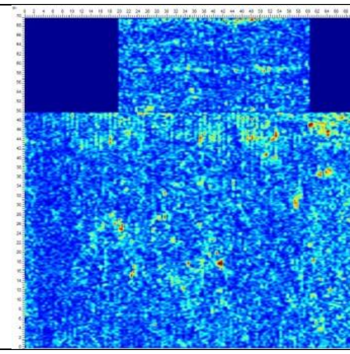
120cm-130cm	**130cm-140cm**	**140cm-150cm**
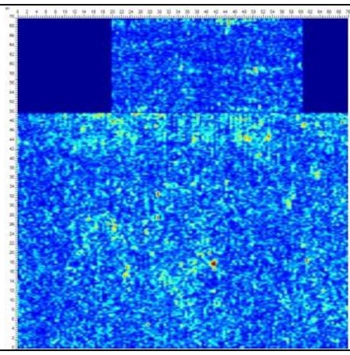	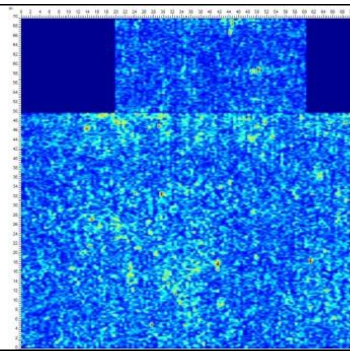	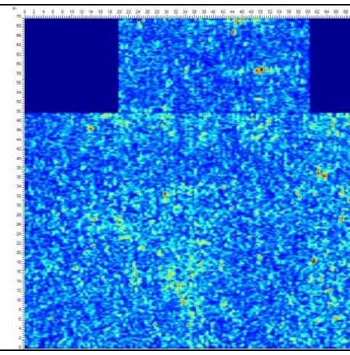
150cm-160cm	**160cm-170cm**	**170cm-180cm**
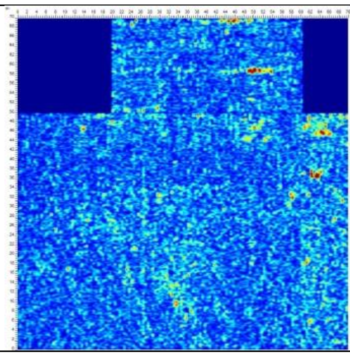	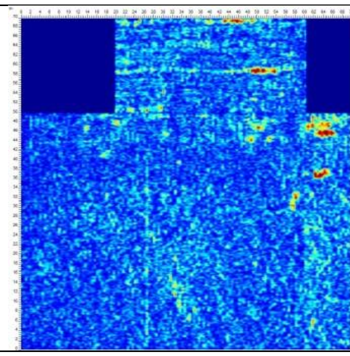	
180cm-190cm	**190cm-200cm**	

Table 1: GPR depth slices for the grids with code names Amlyros2_0 to Almyros2_4 at Almyros with 10 cm thickness.

Figure 15 illustrates a representative GPR slice that is superimposed on the magnetic results. In total, five groups of linear anomalies are identified and due to their geometry, they can be assigned to buried walls. The anomaly described by A5 reveals a structure that appears misplaced regarding the magnetic results, but it has the same orientation. In contrast, while anomalies A1, A3 and A4 seem to meet the same position with the corresponding magnetic anomalies, they exhibit different orientation. Finally, anomaly A2 could be interpreted as walls forming the corner of a house; however, this feature is not visible on the magnetic data (Figure 16).

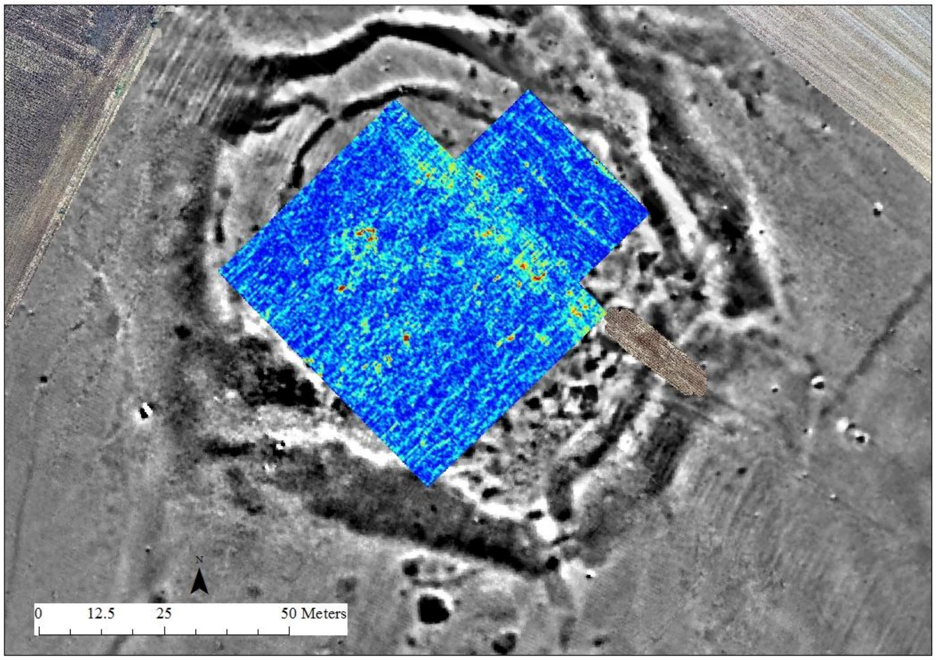

Figure 15: GPR slice at 90-100cm depth at the top of the magoula at Almyros 2.

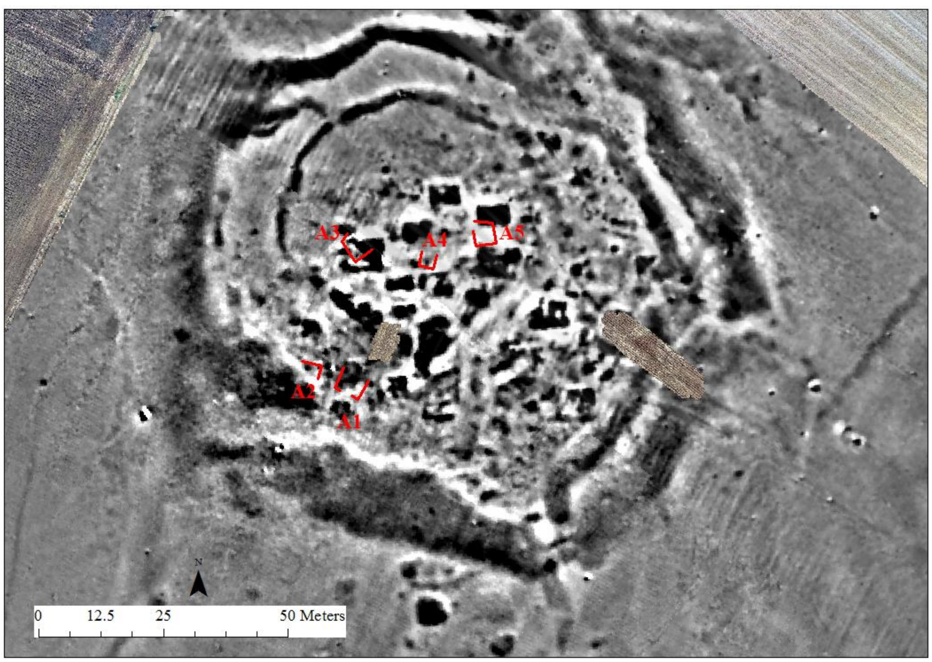

Figure 16: GPR interpretation (red color) that is superimposed on the magnetic results.

Resistance Survey

Resistivity survey at Alymros 2 was conducted in two areas: one investigating the area at the center of the magoula and the other focusing on the potential boundary of the settlement (Figure 17). At the center, we observe three anomalies with high resistance also visible in the geomagnetic data (B9, B10, and B12). Likewise, B8 and B6 also are visible in the resistivity data although they are less visible. However, the squareish resistive area is not well compatible with the magnetic data, as substantial anomaly B7 is almost invisible in this survey, creating an anomalous case. Furthermore, other magnetically visible anomalies, such as the B21 to the east, are also not visible.

In the second survey area, we observe a clear low-boundary division between some highly resistive areas, potentially indicating a "void" area. A resistive area to the west has an extension in an east-west direction, cutting the potential ditch A2. Resistive areas to the east are only partially visible in the data so that little argument can be made.

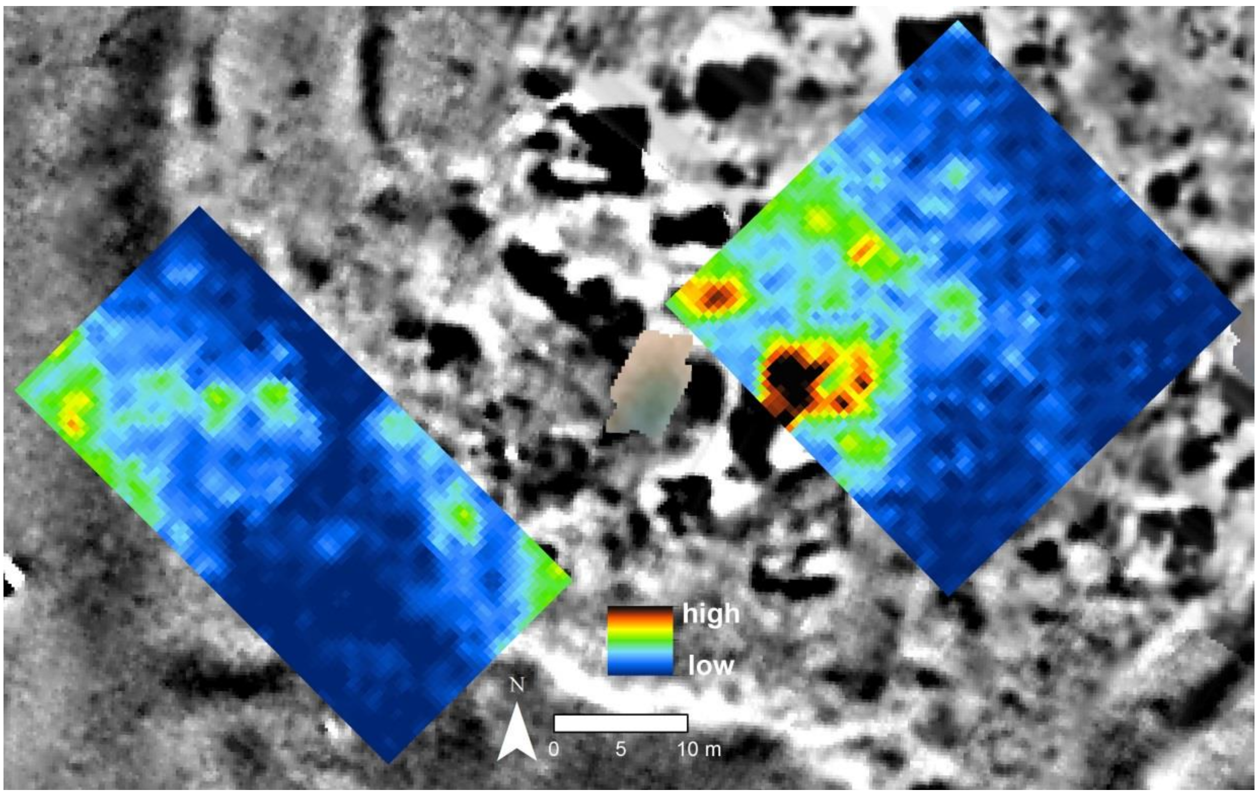

Figure 17: Results of the resistance survey over geomagnetic results

Integration of Geophysical Results

At Almyros 2 various geophysical methodologies were applied for the prospection of the site, including magnetic (SENSYS), GPR (Noggin Plus 250 MHz), resistivity (Geoscan RM85) and soil conductivity/magnetic susceptibility (Geophex GEM2) (Figure 18). Most of the useful information regarding the cultural landscape of Almyros 2 came from the SENSYS magnetic gradiometry survey and the GEM-2 measurements. Surprisingly, the GPR survey was not able to provide any significant reflectors and even the resistivity survey was marginally helpful in verifying just a couple of candidate targets suggested by the magnetic survey of the site.

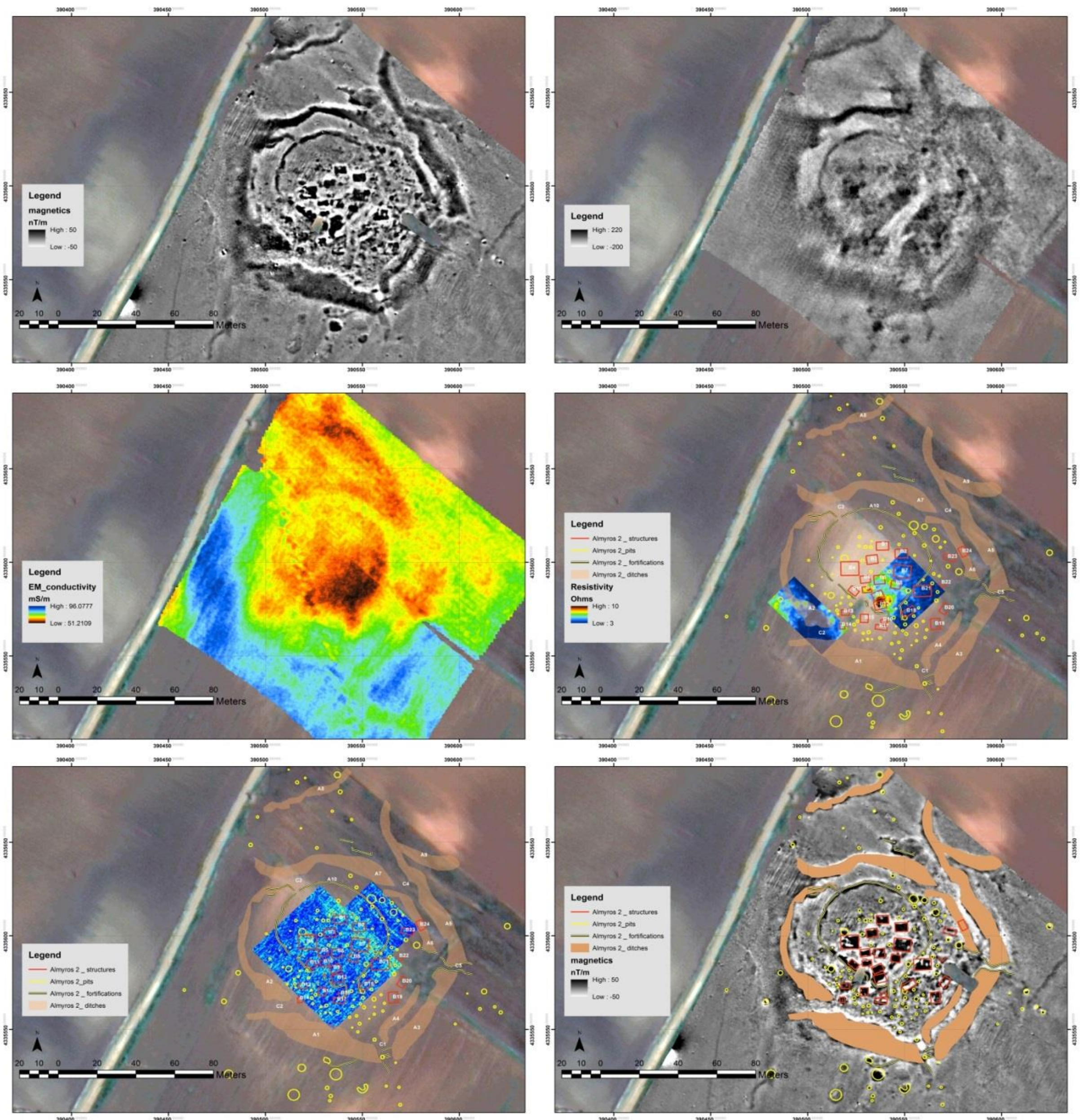

Figure 18: Comparison of the results from the geophysical survey

The extent of the settlement does not seem to be confined within the limits of the tell, which has an oval shape of dimensions 54 x 48 sq m (Figure 19). Instead, the settlement spreads out towards the south outside the core habitation zone (as a consequence of the evolution of the population growth?). The inner oval enclosure (A10) is probably related to a fortification wall of about 1.5 m in width. The outer enclosures are much wider and show a fragmented picture. As shown from magnetic and EM magnetic susceptibility measurements, these features (A1, A2, A3, and A5) are probably related to flood deposits of variable width (wider in the east and south directions spanning from 7-14 m). Especially to the east and to the north, there are signs of an intermediate ditch (A4, A6, and A7) of smaller width. More ditches (A8 and A9) are presented towards the north, with A9 having a semicircular shape, which if projected as a full circle it would enclose an area that appears as a soil mark, similar to the one that the main settlement has left on the satellite and aerial images. Due to the fact that the geophysical measurements did not expand towards this area, it leaves open the hypothesis of the existence of another (satellite) settlement in immediate vicinity of the main habitation zone or the presence of a palaeochannel.

Along the perimeter of the outside ditches there are definite signs of tangential oriented exits/entrances (C1, C2, C3, C4 and C5) that lead away from the settlement. Exits C2 and C3 to the east are much wider than the rest, having a width of about 3.5-6.5 m. Radially outwards and narrower in width are the entrances C1 and C5 to the south and to the east. Entrance C1 has a distinct interest as there are indications of a passage (bridge?) over the outer ditch.

Figure 19: A wider look to the geomagnetic results

At least 12 rectilinear structures (B1-B12) are outlined within the limits of the fortifications, most of which are oriented in a N-S direction. Two of the largest structures (B4 and B7 with approximate dimensions 7 x 9 sq m) are located to the SE and SW sides of the settlement, while the smallest structures (B5, B8, and B11) have dimensions of 5 x 3 sq m. Structures B10 and B12 were verified through soil resistance measurements and produced high resistance anomalies. A weaker signal was produced for structures B6, B9 and B8, while magnetic anomalies B7, B18 and B21 were almost insignificant in terms of their soil resistance signature, probably due to the increased soil deposits east of the settlement. All indications suggest that structures are made of mudbrick and were burnt either intentionally or unintentionally. About half of the area that is confined within the fortifications (about 1000 sq m) consists of an unfilled space with no evidence of any constructions within it. This area is clearly distinguished to the north compared to the built landscape to the south. The magnetic data indicate a wide exit towards the south, and more structural remains (B13-B24) indicate sprawl towards the south and east between the enclosure walls and the surrounding ditches. Buildings B19 and B24 seem to have the largest dimensions. Most of the vertical magnetic gradient targets are also verified through the EM magnetic susceptibility measurements. In addition, the number of isolated magnetic anomalies, most of which could be identified with pits, is increasing towards the south (Figure 20).

The flooding simulation indicates that the first frontier was expected to arrive towards ditch A8 to the north, whereas a rising water level by 2-3 m reaches ditches A2, A5, and A7 at the northern side before it goes around the whole magoula (Figure 21). In contrast, the current EM soil conductivity measurements indicate an impoundment of soil moisture towards the southern direction of the magoula, which justifies also the fuzzy signature of the ditches here. On the whole, Almyros 2 indicates an aggregated settlement that seems to expand outside the core of the habitation zone to the south with an obvious susceptibility to flooding episodes.

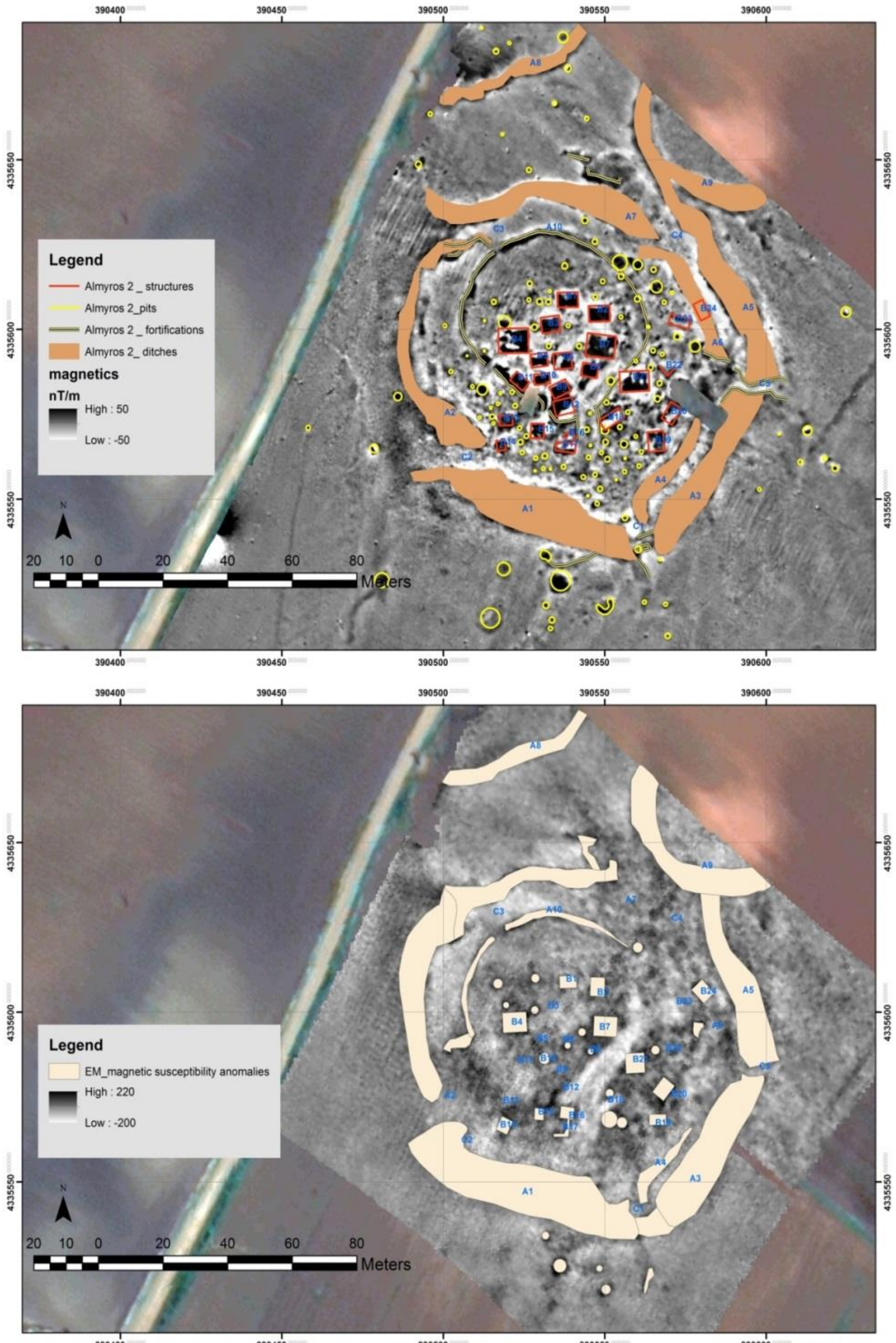

Figure 20. A comparison of geomagnetic and electromagnetic results and corresponding anomalies.

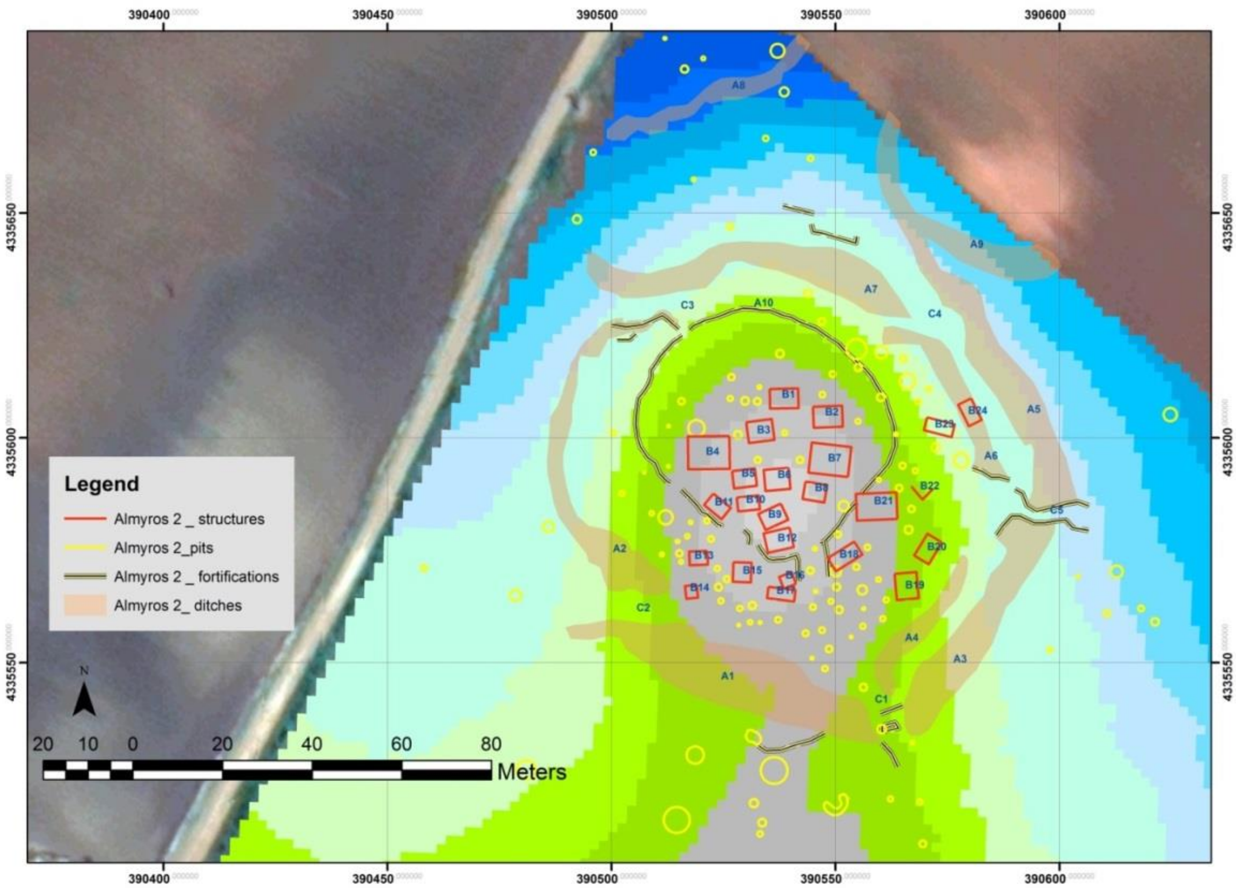

Figure 21: Results of the flooding simulation

Figure 22 A virtual reconstruction of Almyros 2, based on the results of geomagnetic prospection

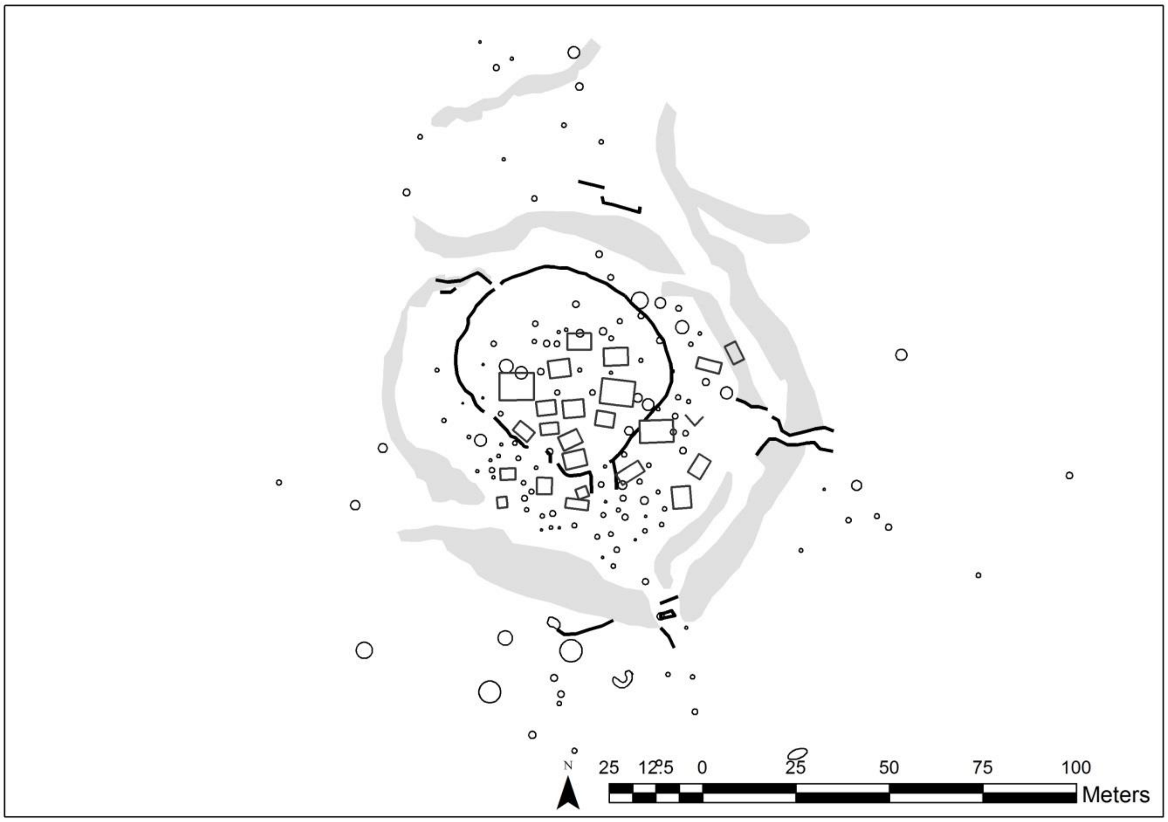

Figure 23. Diagrammatic interpretation of all the geophysical anomalies.

Site Bibliography

Βουζαξάκης, Κ. 2008. *Γεωγραφικά πρότυπα και θεωρίες του διακοινοτικού χώρου στη Νεολιθική Θεσσαλία*. Διδακτορική Διατριβή. Τμήμα Ιστορίας και Αρχαιολογίας. Α.Π.Θ. http://invenio.lib.auth.gr/ record/114226?ln=el , 280-281.

Βουζαξάκης Κ., 2009. *Νεολιθικές θέσεις στη Μαγνησία. Ανασκόπηση – Ανασύνθεση δεδομένων,* στο Αρχαιολογικό Έργο Θεσσαλίας και Στερεάς Ελλάδας 2 (2006), τ. Ι, σελ. 65.

Halstead P., 1984. Strategies of survival: an ecological approach to social and economic change in the early farming communities of Thessaly, N. Greece, Cambridge, (PhD Thesis)., 234 (no 65)

Reinders, H.R. 2004 (ed). *Prehistoric Sites at the Almiros and Sourpi Plains (Thessaly Greece)*. Koninklijke van Gorcum. Assen., 24-25

Wace A.J.B. – Thompson M.S., 1912. *Prehistoric Thessaly*, Cambridge., 10, (no. 65)

Wijnen M. – Rondiri V., 2004b. *Ceramics from Magoula Ambelia – Almirou*, in Reinders 2004, 25-38.